Electrochemical and in-situ X-ray diffraction studies of Ti3C2Tx MXene in ionic liquid electrolyte

Zifeng Lin, Patrick Rozier, Benjamin Duployer, Pierre-Louis Taberna, Babak Anasori, Yury Gogotsi, Patrice Simon

Electrochemical and *in-situ* X-ray diffraction studies of $Ti_3C_2T_x$ MXene in ionic liquid electrolyte

Zifeng Lin [a,b], Patrick Rozier [a,b], Benjamin Duployer [a], Pierre-Louis Taberna [a,b], Babak Anasori [c], Yury Gogotsi [c], Patrice Simon [a,b,*]

[a] CIRIMAT, Université de Toulouse, CNRS, INPT, UPS, 118, Route de Narbonne, 31062 Toulouse cedex 9, France
[b] Reseau sur le Stockage Electrochimique de l'Energie (RS2E) FR CNRS, 3459, France
[c] Department of Materials Science & Engineering, A.J. Drexel Nanomaterials Institute, Drexel University, Philadelphia, PA 19104, USA

A B S T R A C T

2D titanium carbide ($Ti_3C_2T_x$ MXene) showed good capacitance in both organic and neat ionic liquid electrolytes, but its charge storage mechanism is still not fully understood. Here, electrochemical characteristics of $Ti_3C_2T_x$ electrode were studied in neat EMI-TFSI electrolyte. A capacitive behavior was observed within a large electrochemical potential range (from −1.5 to 1.5 V *vs.* Ag). Intercalation and de-intercalation of EMI^+ cations and/or $TFSI^-$ anions were investigated by *in-situ* X-ray diffraction. Interlayer spacing of $Ti_3C_2T_x$ flakes decreases during positive polarization, which can be ascribed to either electrostatic attraction effect between intercalated $TFSI^-$ anions and positively charged $Ti_3C_2T_x$ nanosheets or steric effect caused by de-intercalation of EMI^+ cations. The expansion of interlayer spacing when polarized to negative potentials is explained by steric effect of cation intercalation.

Keywords:
Supercapacitor
Ti_3C_2
In-situ XRD
Ionic liquid
MXene
2D carbide

1. Introduction

MXenes are two-dimensional (2D) early transition metal carbides and nitrides with a formula of $M_{n+1}X_nT_x$, where M is an early transition metal, X is carbon and/or nitrogen and T represents the surface terminations (=O, -F or -OH), and $n = 1–3$ [1–5]. MXenes have been extensively studied as the electrode materials for electrochemical capacitors (ECs) [6–9] and batteries [10–13]. Though a high volumetric capacitance exceeding 900 F cm^{-3} was achieved in aqueous electrolytes [8], the use of MXenes in organic and ionic liquid electrolytes was reported only recently [14,15]. The first investigation of $Ti_3C_2T_x$ operating in 1-ethyl-3-methylimidazolium bis-(trifluoromethylsulfonyl)-imide (EMI-TFSI) neat ionic liquid was reported with a capacitance of 70 F g^{-1} within a voltage window of 3V [15]. However, the charge storage mechanism remains unclear as reversible peaks appear in cyclic voltammograms. In aqueous electrolytes, such redox peaks have been ascribed to the pseudocapacitive reactions of surface functional groups of MXenes [16]. A pseudocapacitive contribution originating from redox reactions of Ti in H_2SO_4 electrolyte was also shown [17]. However, surface functional groups (O or F) and Ti are not supposed to be electrochemically active in aprotic ionic liquids. Intercalation of cations between MXene layers from aqueous electrolytes was observed by *in-situ* XRD [6], and similar intercalation behavior was reported for MXene battery electrodes [18,19]. It is reasonable to assume that intercalation may occur in ionic liquid electrolytes as well.

In this work, *in-situ* XRD technology was combined with electrochemical characterizations to provide insights into the charge storage mechanism of $Ti_3C_2T_x$ in EMI-TFSI ionic liquid electrolyte.

2. Experimental

The preparation of the delaminated $Ti_3C_2T_x$ was described elsewhere [8]. Briefly, 2 g lithium fluoride was added to 40 mL 9 M hydrochloric acid solution, followed by the slow addition of 2 g of Ti_3AlC_2. After etching for 30 h at 35 °C, the obtained $Ti_3C_2T_x$ flakes were washed until a pH value around 6. The delaminated $Ti_3C_2T_x$ colloidal solution was then obtained by 1-h sonication and collected after 1-h centrifugation at 3500 rpm to eliminate the sediment. $Ti_3C_2T_x$ film with intercalated water (denoted as $Ti_3C_2T_x$ film) was prepared by vacuum-assisted filtration of the delaminated $Ti_3C_2T_x$ colloidal solution and peeled off in acetone. After immersing in EMI-TFSI (Sigma-Aldrich) electrolyte for 72 h, a free-standing $Ti_3C_2T_x$ film with intercalated EMI-TFSI ionic liquid (denoted as IL-$Ti_3C_2T_x$ film) with a mass loading of 0.76 mg cm^{-2} was achieved, then transferred to a vacuum oven for drying at 80 °C for 48 h to remove the residual water.

* Corresponding author at: CIRIMAT, Université de Toulouse, CNRS, INPT, UPS, 118, Route de Narbonne, 31062 Toulouse cedex 9, France.
E-mail address: simon@chimie.ups-tlse.fr (P. Simon).

http://dx.doi.org/10.1016/j.elecom.2016.08.023 .

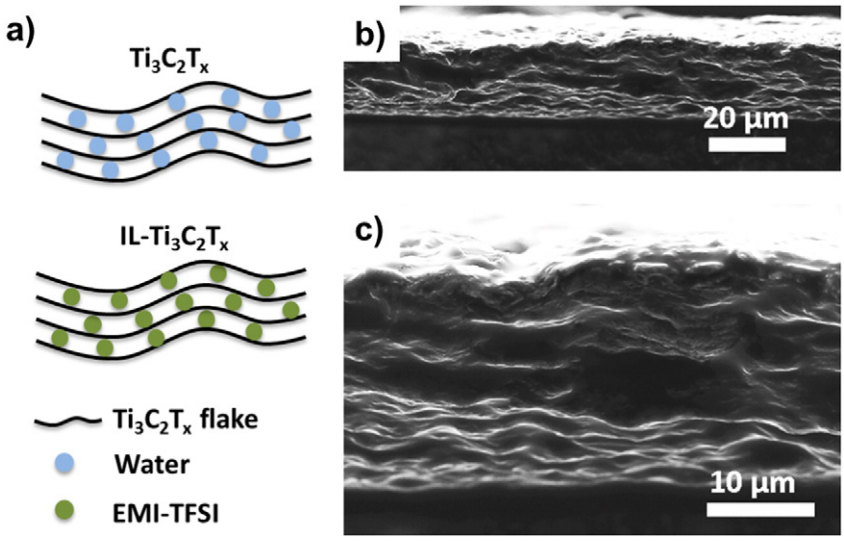

Fig. 1. a) The schematic of $Ti_3C_2T_x$ and IL-$Ti_3C_2T_x$ films; b, c) cross-sectional SEM images of IL-$Ti_3C_2T_x$ film.

IL-$Ti_3C_2T_x$ films were used as electrodes directly without any binders with EMI-TFSI neat ionic liquid as the electrolyte. Three-electrode Swagelok symmetric cells were assembled and tested at room temperature using a VMP3 potentiostat (Biologic, USA.). Two layers of separator (Celgard@ 3501) were used together with platinum discs as current collectors and a silver wire as a quasi-reference electrode. A two-electrode cell was used for *in-situ* XRD study [20]. A freestanding MXene film working electrode was placed onto a beryllium foil acting as the current collector without any binders and an over-capacitive activated carbon (YP50, Kuraray, Japan) was used as the counter electrode with a Pt current collector. Before starting the *in-situ* XRD test, cyclic voltammetry (CV) scanning with a rate of 20 mV s^{-1} was conducted for 50 cycles to stabilize the electrochemical signature. All cells were assembled in a glove box under argon atmosphere with water and oxygen contents less than 1 ppm.

Thermogravimetric measurements (TGA) of IL-$Ti_3C_2T_x$ were conducted under nitrogen atmosphere, after 48 h vacuum drying, from room temperature up to 1000 °C with a heating rate of 3 °C per minute. *In-situ* XRD patterns of the $Ti_3C_2T_x$ electrodes were recorded with a Bruker D8 (Bruker, Germany) diffractometer using Cu K_α radiation ($\lambda = 0.154$ nm) in the 5–50° 2θ range with a step of 0.0152°. XRD measurements were made at constant potential, after 1-h polarization to reach the steady state.

Electrochemical impedance spectroscopy (EIS) measurements were carried out at constant potentials (after 1-h constant polarization to reach the steady-state) with amplitude of 10 mV at the frequency range from 200 kHz to 0.01 Hz. The mean capacitance was calculated from the CV at a scan rate of 1 mV s^{-1}. Specifically, the discharge current was integrated with potential, then divided by the potential window and scan rate, and normalized by mass.

3. Results and discussion

The schematic (Fig. 1 a) presents the $Ti_3C_2T_x$ and IL-$Ti_3C_2T_x$ films that are pre-intercalated with water and EMI-TFSI ionic liquid respectively, which are expected to prevent restacking of $Ti_3C_2T_x$ nanosheets. The cross-sectional view of an IL-$Ti_3C_2T_x$ film with a layered structure (Fig. 1 b and c) shows a wavy pattern of MXene layers.

The thermograms of IL-$Ti_3C_2T_x$ film, recorded under nitrogen atmosphere (Fig. 2a) show no mass loss below 250 °C, thus evidencing the complete removal of water and acetone after vacuum drying. About 80% of the mass is lost between 300 °C and 500 °C corresponding mainly to the decomposition of the EMI-TFSI ionic liquid from the IL-$Ti_3C_2T_x$ film [21] with a possible contribution from loss of surface functional groups of MXene [22].

Fig. 2b shows the cyclic voltammograms (CVs) of IL-$Ti_3C_2T_x$ film in neat EMI-TFSI electrolyte. The symmetric CV shape reveals a capacitive behavior with a mean specific capacitance of 84 F g^{-1} within a potential range from −1.5 V to 1.5 V *vs.* Ag. Two pairs of noticeable peaks with small voltage offsets in both positive (around −0.2 V) and negative (around 0.6 V) potential ranges can be observed. The peak potential difference increases with the potential scan rate but the process remains reversible; a similar behavior was also reported for 2D *T*-Nb_2O_5, where an intercalation pseudocapacitance charge storage mechanism was involved [23]. Here, a non-random intercalation of EMI^+ cations and/or $TFSI^-$ anions between stacked $Ti_3C_2T_x$ flakes is assumed to cause the peaks in negative and positive ranges, respectively. Fig. 2c shows the Coulombic efficiency above 95%, suggesting a highly reversible behavior. However, capacitance decreases to 76% of the initial value after 1400 cycles.

In-situ XRD analysis was performed to understand the charge storage mechanism. The *in-situ* XRD diffraction patterns of IL-$Ti_3C_2T_x$ film

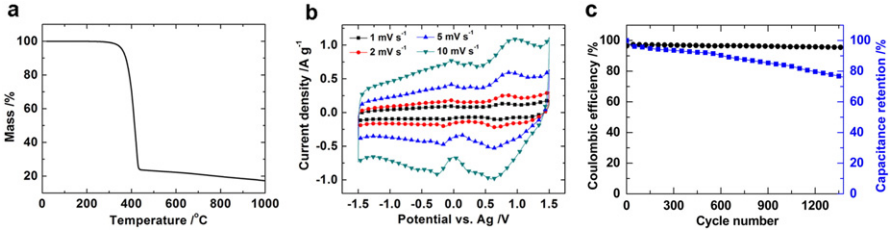

Fig. 2. a) Thermogravimetric analysis (TGA) of IL-$Ti_3C_2T_x$ film from room temperature to 1000 °C; b) cyclic voltammetry profiles at various scan rates from 1 to 10 mV s^{-1} within a potential range from −1.5 V to 1.5 V *vs.* Ag in EMI-TFSI electrolyte; c) Coulombic efficiency and capacitance retention *vs.* cycle number.

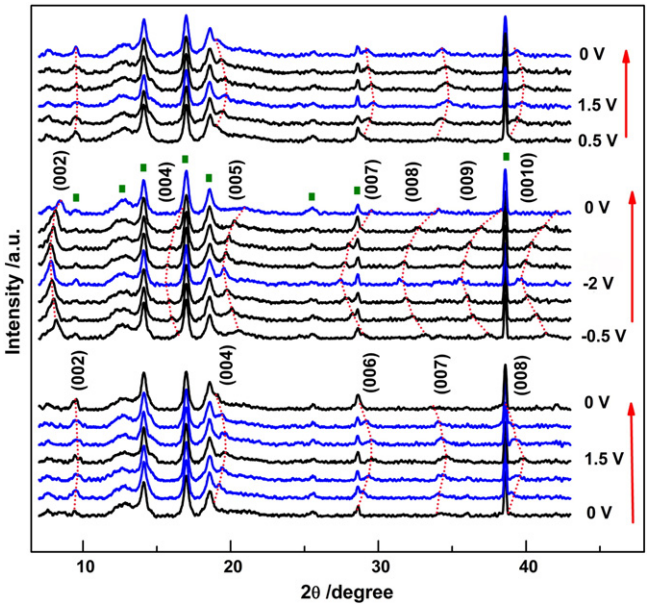

Fig. 3. Electrochemical *in-situ* X-ray diffraction study of IL-$Ti_3C_2T_x$ film at various constant potentials (0.5 V steps) in EMI-TFSI electrolyte. Green squares represent peaks of the *in-situ* XRD cell without working electrode. The arrows show the potential scanning direction and the red dashed lines show the shift of $Ti_3C_2T_x$ peaks.

were recorded at various potentials as shown in Fig. 3. The (005), (007) and (009) peaks, which have not been reported in previous studies, were identified suggesting the loss of symmetry in some stacking layers. Such behavior is similar to 1H to 1T phase transition of MoS_2 during Na^+ insertion, as reported elsewhere [24]. Comparing the patterns in positive and negative potential ranges, two different sets of diffraction peaks are observed, suggesting that different processes are involved under positive and negative potential ranges. Under a positive potential range, a progressive and continuous shift of the $Ti_3C_2T_x$ (*00l*) peaks to higher 2θ values is observed with increased applied potential (from 0 V to 1.5 V), corresponding to a continuous decrease of interlayer spacing. Then the peaks reversibly shift back to their original 2θ position when discharged from 1.5 V back to 0 V, indicating the increase of interlayer spacing. As the change of interlayer spacing can be induced by both electrostatic or steric effects during ion intercalation [6,25–28], the reduction of interlayer spacing with increasing applied potential within the positive potential range can be explained in two ways: 1) electrostatic attraction between intercalated $TFSI^-$ anions and positively charged $Ti_3C_2T_x$ layers; 2) steric effects caused by the de-intercalation of EMI^+ cations, which has been reported in both aqueous and organic electrolytes elsewhere [14,29]. The exact identification of origins of the observed dimensional change can possibly be done by using electrochemical quartz crystal microbalance (EQCM) [29] or *in-situ* nuclear magnetic resonance (NMR). In the negative potential range, the appearance of the (002) peak at a lower 2θ degree position can be ascribed to the pillared structure of $Ti_3C_2T_x$ flakes when intercalated by EMI^+ cations, which has already been observed for MXene [9,14] and other 2D materials [30,31]. Increasing peak intensity when polarized to the negative potentials also confirms the pillaring effect caused by EMI^+ intercalation. The continuous shift of the $Ti_3C_2T_x$ peaks to lower 2θ values occurs with decreasing applied potential, evidencing an increased interlayer spacing that is consistent with previous observations for MXene electrodes in aqueous supercapacitors [6] and metal-ion capacitors [32,33]. The maximum interlayer spacing was obtained at −2 V that is the highest negative overpotential. EMI^+ intercalation has been confirmed in $Ti_3C_2T_x$ when using organic electrolyte [14]. Since, the electrostatic effect will cause reduction in interlayer spacing, the expansion of interlayer spacing should be explained by the steric effect caused by EMI^+ cation intercalation. After the negative polarization, the sample was polarized back positively (see Fig. 3, top). The (002) peak initially observed at 8.5 2θ degree at 0 V shifts to 9.5° when polarized to 0.5 V, which is the same position as measured during the first positive polarization (Fig. 3, bottom), evidencing a reversible transition between positive and negative polarizations.

Overall, the charge storage mechanism in $Ti_3C_2T_x$ with EMI-TFISI electrolyte can be described as following: under positive polarization, the electrostatic attraction between intercalated $TFSI^-$ anions and positively charged MXene layers and/or steric effect originating from de-intercalation of EMI^+ cations lead to a decrease of the interlayer spacing. In opposite, the steric effect of EMI^+ cation intercalation accounts for the observed increase of the interlayer spacing under negative polarization.

The fast increase of the imaginary part of all Nyquist plots at low frequencies (Fig. 4) evidences a capacitive storage mechanism. The electrode resistance R_i at various potentials was calculated from the difference between knee frequency resistance (see dashed lines in Fig. 4a) and the high frequency resistance (where the imaginary part is null). R_i corresponds to the ionic resistance of the electrolyte confined inside the 2D $Ti_3C_2T_x$ structure. As can be seen in Fig. 4b, the ionic liquid resistance under positive potentials is higher than in the negative potential range, demonstrating a slower ion motion during positive polarization. This is consistent with the XRD data that showed a more compact structure with decreasing interlayer spacing under positive polarization, which is believed to reduce the ion motion.

4. Conclusions

A $Ti_3C_2T_x$ film intercalated with ionic liquid was prepared and electrochemically characterized in EMI-TFSI ionic liquid electrolyte. A capacitive behavior within a wide potential range from −1.5 to 1.5 V *vs.* Ag has been demonstrated. The interlayer spacing increased with

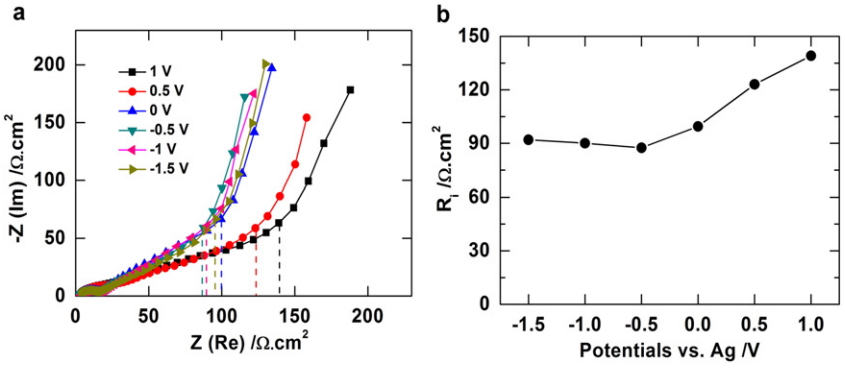

Fig. 4. a) Nyquist plot of IL-$Ti_3C_2T_x$ at different potentials *vs.* Ag. The dashed lines show the resistances at the knee frequencies. b) Ionic liquid diffusion resistance in $Ti_3C_2T_x$ electrodes.

positive polarization and decreased with negative polarization as shown by *in-situ* XRD test. The shrinkage of interlayer spacing in the positive potential range was induced by 1) electrostatic attraction between the intercalated $TFSI^-$ anions and positively-charged $Ti_3C_2T_x$ surface and/or 2) steric effect of EMI^+ cation de-intercalation. Under negative potentials, the EMI^+ cations intercalation accounts for the expansion of interlayer spacing.

5. Acknowledgements

We thank Y. Dall'Agnese for help with in *in-situ* XRD experiments and A. Brahmi for TGA analysis (from Université de Toulouse). Z. F. Lin was supported by China Scholarship Council (NO. 201304490006). P. Simon acknowledges the support from European Research Council (ERC, Advanced Grant, ERC-2011-AdG, and Project no. 291543-IONACES). The French Research Federation Fermat FR3089 is acknowledged for providing XRD facility. Work at Drexel University was supported as part of the Fluid Interface Reactions, Structures and Transport (FIRST) Center, an Energy Frontier Research Center funded by the U.S. Department of Energy, Office of Science, Office of Basic Energy Sciences.

References

[1] M. Naguib, V.N. Mochalin, M.W. Barsoum, Y. Gogotsi, 25th anniversary article: MXenes: a new family of two-dimensional materials, Adv. Mater. 26 (2014) 992–1005.
[2] M. Naguib, M. Kurtoglu, V. Presser, J. Lu, J. Niu, M. Heon, L. Hultman, Y. Gogotsi, M.W. Barsoum, Two-dimensional nanocrystals produced by exfoliation of Ti_3AlC_2, Adv. Mater. 23 (2011) 4248–4253.
[3] P. Urbankowski, B. Anasori, T. Makaryan, D. Er, S. Kota, P.L. Walsh, M. Zhao, V.B. Shenoy, M.W. Barsoum, Y. Gogotsi, Synthesis of two-dimensional titanium nitride Ti_4N_3 (MXene), Nanoscale 8 (2016) 11385–11391.
[4] M. Naguib, Y. Gogotsi, Synthesis of two-dimensional materials by selective extraction, Acc. Chem. Res. 48 (2015) 128–135.
[5] Y. Gogotsi, Chemical vapour deposition: transition metal carbides go 2D, Nat. Mater. 14 (2015) 1079–1080.
[6] M.R. Lukatskaya, O. Mashtalir, C.E. Ren, Y. Dall Agnese, P. Rozier, P.L. Taberna, M. Naguib, P. Simon, M.W. Barsoum, Y. Gogotsi, Cation intercalation and high volumetric capacitance of wo-dimensional titanium carbide, Science 341 (2013) 1502–1505.
[7] M. Hu, Z. Li, H. Zhang, T. Hu, C. Zhang, Z. Wu, X. Wang, Self-assembled $Ti_3C_2T_x$ MXene film with high gravimetric capacitance, Chem. Commun. 51 (2015) 13531–13533.
[8] M. Ghidiu, M.R. Lukatskaya, M.-Q. Zhao, Y. Gogotsi, M.W. Barsoum, Conductive two-dimensional titanium carbide 'clay' with high volumetric capacitance, Nature 516 (2014) 78–81.
[9] X. Wang, S. Kajiyama, H. Iinuma, E. Hosono, S. Oro, I. Moriguchi, M. Okubo, A. Yamada, Pseudocapacitance of MXene nanosheets for high-power sodium-ion hybrid capacitors, Nat. Commun. 6 (2015), 6544.
[10] C.E. Ren, M. Zhao, T. Makaryan, J. Halim, M. Boota, S. Kota, B. Anasori, M.W. Barsoum, Y. Gogotsi, Porous two-dimensional transition metal carbide (MXene) flakes for high-performance Li-ion storage, ChemElectroChem 3 (2016) 689–693.
[11] D. Er, J. Li, M. Naguib, Y. Gogotsi, V.B. Shenoy, Ti_3C_2 MXene as a high capacity electrode material for metal (Li, Na, K, Ca) ion batteries, ACS Appl. Mater. Interfaces 6 (2014) 11173–11179.
[12] M. Naguib, J. Halim, J. Lu, K.M. Cook, L. Hultman, Y. Gogotsi, M.W. Barsoum, New two-dimensional niobium and vanadium carbides as promising materials for Li-ion batteries, J. Am. Chem. Soc. 135 (2013) 15966–15969.
[13] M. Naguib, J. Come, B. Dyatkin, V. Presser, P.-L. Taberna, P. Simon, M.W. Barsoum, Y. Gogotsi, MXene: a promising transition metal carbide anode for lithium-ion batteries, Electrochem. Commun. 16 (2012) 61–64.
[14] Y. Dall'Agnese, P. Rozier, P.-L. Taberna, Y. Gogotsi, P. Simon, Capacitance of two-dimensional titanium carbide (MXene) and MXene/carbon nanotube composites in organic electrolytes, J. Power Sources 306 (2016) 510–515.
[15] Z. Lin, D. Barbara, P.-L. Taberna, K.L. Van Aken, B. Anasori, Y. Gogotsi, P. Simon, Capacitance of $Ti_3C_2T_x$ MXene in ionic liquid electrolyte, J. Power Sources 326 (2016) 575–579.
[16] Y. Dall'Agnese, M.R. Lukatskaya, K.M. Cook, P.L. Taberna, Y. Gogotsi, P. Simon, High capacitance of surface-modified 2D titanium carbide in acidic electrolyte, Electrochem. Commun. 48 (2014) 118–122.
[17] M.R. Lukatskaya, S.M. Bak, X.Q. Yu, X.Q. Yang, M.W. Barsoum, Y. Gogotsi, Probing the mechanism of high capacitance in 2D titanium carbide using in situ X-ray absorption spectroscopy, Adv. Energy Mater. 5 (2015) 1500589.
[18] X.F. Wang, X. Shen, Y.R. Gao, Z.X. Wang, R.C. Yu, L.Q. Chen, Atomic-scale recognition of surface structure and intercalation mechanism of $Ti_3C_2T_X$, J. Am. Chem. Soc. 137 (2015) 2715–2721.
[19] Y. Xie, Y. Dall'Agnese, M. Naguib, Y. Gogotsi, M.W. Barsoum, H.L. Zhuang, P.R.C. Kent, Prediction and characterization of MXene nanosheet anodes for non-lithium-ion batteries, ACS Nano 8 (2014) 9606–9615.
[20] B. Zhang, R. Dugas, G. Rousse, P. Rozier, A.M. Abakumov, J.-M. Tarascon, Insertion compounds and composites made by ball milling for advanced sodium-ion batteries, Nat. Commun. 7 (2016) 10308.
[21] A.I. Horowitz, M.J. Panzer, High-performance, mechanically compliant silica-based ionogels for electrical energy storage applications, J. Mater. Chem. 22 (2012) 16534–16539.
[22] O. Mashtalir, M.R. Lukatskaya, M.-Q. Zhao, M.W. Barsoum, Y. Gogotsi, Amine-assisted delamination of Nb_2C MXene for Li-ion energy storage devices, Adv. Mater. 27 (2015) 3501–3506.
[23] V. Augustyn, J. Come, M.A. Lowe, J.W. Kim, P.-L. Taberna, S.H. Tolbert, H.D. Abruña, P. Simon, B. Dunn, High-rate electrochemical energy storage through Li^+ intercalation pseudocapacitance, Nat. Mater. 12 (2013) 518–522.
[24] X. Xie, T. Makaryan, M. Zhao, K.L. Van Aken, Y. Gogotsi, G. Wang, MoS_2 nanosheets vertically aligned on carbon paper: a freestanding electrode for highly reversible sodium-ion batteries, Adv. Energy Mater. 6 (2016) 1502161.
[25] H. Kim, D.J. Kim, D.-H. Seo, M.S. Yeom, K. Kang, D.K. Kim, Y. Jung, Ab initio study of the sodium intercalation and intermediate phases in $Na_{0.44}MnO_2$ for sodium-ion battery, Chem. Mater. 24 (2012) 1205–1211.
[26] C.R. Fell, M. Chi, Y.S. Meng, J.L. Jones, In situ X-ray diffraction study of the lithium excess layered oxide compound $Li[Li_{0.2}Ni_{0.2}Mn_{0.6}]O_2$ during electrochemical cycling, Solid State Ionics 207 (2012) 44–49.
[27] M. Okubo, E. Hosono, J. Kim, M. Enomoto, N. Kojima, T. Kudo, H. Zhou, I. Honma, Nanosize effect on high-rate Li-ion intercalation in $LiCoO_2$ electrode, J. Am. Chem. Soc. 129 (2007) 7444–7452.
[28] J. Segalini, E. Iwama, P.-L. Taberna, Y. Gogotsi, P. Simon, Steric effects in adsorption of ions from mixed electrolytes into microporous carbon, Electrochem. Commun. 15 (2012) 63–65.
[29] M.D. Levi, M.R. Lukatskaya, S. Sigalov, M. Beidaghi, N. Shpigel, L. Daikhin, D. Aurbach, M.W. Barsoum, Y. Gogotsi, Solving the capacitive paradox of 2D MXene using electrochemical quartz-crystal admittance and in situ electronic conductance measurements, Adv. Energy Mater 5 (2015) 1400815.
[30] M.M. Hantel, R. Nesper, A. Wokaun, R. Kötz, In-situ XRD and dilatometry investigation of the formation of pillared graphene via electrochemical activation of partially reduced graphite oxide, Electrochim. Acta 134 (2014) 459–470.
[31] H. Li, G. Zhu, Z. Yang, Z. Wang, Z.-H. Liu, Preparation and capacitance property of MnO_2-pillared Ni^{2+}–Fe^{3+} layered double hydroxides nanocomposite, J. Colloid Interface Sci. 345 (2010) 228–233.
[32] J. Come, M. Naguib, P. Rozier, M.W. Barsoum, Y. Gogotsi, P.-L. Taberna, M. Morcrette, P. Simon, A non-aqueous asymmetric cell with a Ti_2C-based two-dimensional negative electrode, J. Electrochem. Soc. 159 (2012) A1368–A1373.
[33] Y. Dall'Agnese, P.-L. Taberna, Y. Gogotsi, P. Simon, Two-dimensional vanadium carbide (MXene) as positive electrode for sodium-ion capacitors, J. Phys. Chem. Lett. 6 (2015) 2305–2309.